Soft Switching Loss Measurements of a 1.2 kV SiC MOSFET Module by both Electrical and Calorimetric Methods for High Frequency Applications

S. Tiwari[1], J. K. Langelid[2], O.-M. Midtgård[1], and T. M. Undeland[1]

[1]Norwegian University of Science and Technology
7491 Trondheim, Norway
subhadra.tiwari@ntnu.no

[2]EFD Induction AS
N-3701 Skien, Norway
John.Langelid@efd-induction.com

Acknowledgments

The authors would like to thank The Research Council of Norway and 6 industry partners who sponsor this project: EFD Induction, Siemens, Eltek, Statkraft, Norwegian Electric Systems, and Vacon.

Keywords

≪Silicon Carbide (SiC)≫, ≪MOSFET≫, ≪Soft switching≫, ≪Resonant converter≫, ≪Conduction losses≫, ≪Switching losses≫, ≪Efficiency≫.

Abstract

This paper investigates the soft switching performance of a 1.2 kV half-bridge SiC MOSFET module, FCA150XB120 from Sanrex. The selected module has both MOSFET and diode integrated on a single chip. A single pulse control circuit is employed in a half-bridge series resonant inverter topology with a split dc-link and an LC load in order to emulate a real inverter operation. This results in a square wave output voltage and a sine wave output current where the switching is performed before the zero crossing of current (an inductive mode). In addition, a calorimetric loss measurement is carried out in a 78 kW full-bridge resonant inverter switching at about 200 kHz yielding an efficiency of 99 %. Moreover, this paper aims to find the highest possible switching frequency achievable with the selected module. Besides, the electrically measured loss is compared with the calorimetrically measured loss and the possible reasons for discrepancies are discussed.

1 Introduction

In a typical datasheet of a power switch such as MOSFET and IGBT, only the hard switching losses are provided [1, 2, 3, 4]. In a hard switched inverter, the switching takes place at high voltage and current resulting in high switching losses, whereas in a soft switched inverter the switching takes place at small voltage and current and thereby low switching losses. However, when an inverter switches at high frequency in the range of 200 kHz to 500 kHz, the switching losses become significant even in a soft switched inverter. Therefore, it is essential to measure the switching losses in such an inverter in order to design the thermal management.

Thus, in this paper, the soft switching losses of a 1.2 kV half-bridge SiC MOSFET module, from Sanrex, FCA150XB120 [4], are measured electrically in a half-bridge series resonant inverter with a single pulse control. In the selected SiC MOSFET module, both MOSFET and anti-parallel diode are fabricated on a single chip unlike in the standard MOSFET module where they are on separate chips. Such a resonant inverter with a split dc-link and an LC load results in an output voltage and a current with a square and sine wave shapes respectively. With a sine wave current, there is possibility to switch at a minimum current. The switching is performed before the zero crossing of current, that is, in an inductive mode of switching, yielding only the turn-off losses.

In addition, the losses in a 78 kW full-bridge series resonant inverter is measured using a calorimetric loss measurement method. The turn-on takes place at zero voltage and turn-off at minimum current by adjusting the blanking time. Subtracting the conduction losses, the turn-off losses are calculated in order to compare the discrepancies in losses obtained from the two measurement methods. Additionally, the loss data also gives insight into the highest possible power or switching frequency (f_{sw}) that can be achieved from an inverter.

There are several publications on the loss measurements with the hard switching of devices [5, 6, 7], but few on that with the soft switching [8, 9, 10]. Additionally, none of the publications have compared the losses between the electrical and calorimetric loss measurements where the main contribution of the paper lies.

The paper is organized as follows. The description of the device under test (DUT) is presented in Section 2. Following this is the circuit topology, methodology and measurement setup for soft switching loss measurement in Section 3, and it has two parts. In the first part, the electrical loss measurement in a half-bridge resonant inverter is analysed, and in the second part, the calorimetric loss measurement in a full-bridge resonant inverter is covered. Then, the measurement results obtained from two measurement techniques are compared and discussed in Section 4. In Section 5, the maximum achievable switching frequency by using the chosen SiC MOSFET module is computed. Finally, the major conclusions are summarized in Section 6.

2 Device under test

A SiC MOSFET module, FCA150XB120, from Sanrex is used in the measurement. Unlike in a standard SiC MOSFET module, where a MOSFET and an anti-parallel diode chips are fabricated separately, in the chosen MOSFET module, both the MOSFET and diode chips are fabricated on a single chip, so this MOSFET is also called DioMOS [11]. Table I shows the major differences between the selected SiC module and the standard SiC module (CAS120M12BM2) taken from the manufacturer datasheet [1, 4]. In FCA150XB120 module, there are three number of chips and in CAS120M12BM2 module, there are six chips. R_{dson} is the on-state resistance, and R_{thjc} is the junction to case thermal resistance of the MOSFET. It should also be noted that the package size of the former module is smaller compared to the latter module. Besides, the solder bonding technique is employed in the previous, whereas that in the latter is wire bonding type. Fig. 1 shows photographs of the DioMOS and the standard SiC MOSFET modules.

Compared to Si devices, SiC devices have relatively lower gate to source threshold voltage (V_{gsth}). Though the input and output capacitances are low in SiC, dv/dt is high. As a consequence, enough charge can be coupled to the gate loop through miller capacitance during turn-off. If negative gate voltage and closed coupled driver layout are not in place, this coupled charge can easily exceed the V_{gsth} limit and can cause malfunction of the device. But, the datasheet of the DioMOS indicates relatively higher V_{gsth} compared to the standard SiC module which is preferable from an application point of view.

Table I: Major differences between a 1.2 kV SiC DioMOS and a 1.2 kV standard SiC MOSFET module.

Parameters / Module	DioMOS FCA150XB120, Sanrex	Standard SiC MOSFET CAS120M12BM2, Wolfspeed
No. of chips $\times$ ($m\Omega$)	3×18	6×80
V_{gsth} (V)	4.5	2.6
R_{dson} ($m\Omega$)	5.3	13
R_{thjc} (°C/W)	0.120	0.125
Bonding	Solder	Wire
Package size	$30 \times 93 \times 14$	$62 \times 106 \times 30$

(a) DioMOS module. (b) Standard SiC MOSFET module.

Fig. 1: Photographs of DioMOS and standard SiC MOSFET modules.

3 Circuit topology, methodology and measurement setup

This section is divided into two subsections. In Subsection 3.1, the electrical loss measurement in a half-bridge resonant inverter is presented and in Subsection 3.2, the calorimetric loss measurement in a full-bridge inverter is covered. As turn-off loss depends significantly on the performance of driver circuit, it is worth mentioning that the same driver is used in case of electrical and calorimetric methods.

3.1 Electrical loss measurement in a half-bridge resonant inverter

The performance of power devices should be evaluated under operating conditions closely resembling those in an actual application in order to obtain realistic data.

However, for the soft switching loss measurement, the same topology as the hard switching (a chopper circuit with an inductive load) is used in [8], where the switch current remains nearly constant over a switching cycle. A resonant inverter is employed with an inductive load in [9] and an LC load in [10]. In the former topology, the switch current has triangular shape whereas the same in the latter has sinusoidal shape.

In a resonant inverter, the shape of output voltage and current are square and sine wave respectively; thus, in this paper, a resonant inverter with the LC load, as depicted in Fig. 2, is used. The upper transistor (T1) is always in on-state except the period where the lower transistor (T2) is in on-state, including some blanking time (t_b). By adjusting t_b, the switching current can be varied according to the value of interest. The remaining abbreviations used in Fig. 2 are t_d: time delay, G_{upper} and G_{lower}: upper and lower gate pulses respectively, $C_{dc-link}$: dc-link capacitance, V_{ds}: drain source voltage, and I_{ds} and I_L: drain source and load currents respectively.

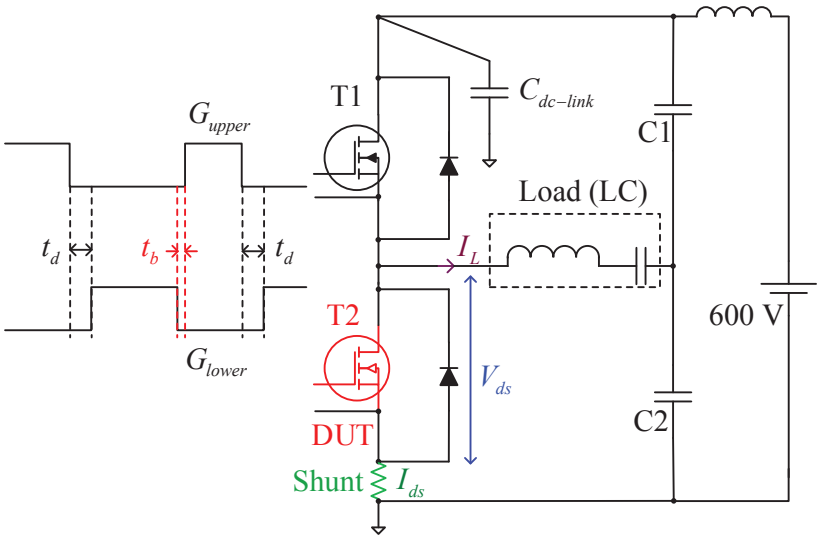

Fig. 2: A half-bridge resonant circuit with LC load for replicating the real soft switching waveforms.

In a soft switching inverter, during the normal operating conditions, there is no significance of having low stray inductance in the switching loop as the device switches with small di/dt. However, during the short circuit conditions, the current is very high and so is the di/dt. The high di/dt combined with switching loop stray inductance cause high voltage overshoot and ringing resulting in EMI and possible device failure. Therefore, it is advisable to maintain lower loop inductances even in a resonant inverter.

Because of this, the dc-link is realized with a planar busbar except the termination parts (needed to facilitate the module connection) so that the stray inductance in the switching loop can be kept as low as possible. A current viewing resistor (CVR, also called a shunt resistor) SSDN - 414 - 01 (400 MHz, 10 $m\Omega$) from T & M research [12] is used for measuring the drain current. The CVR replaces one of the screws in the SiC module as it is mounted directly on the screw terminal. The picture illustrating the placement of the CVR in the laboratory setup is shown in Fig. 3. Fig. 4 a) shows V_{ds}, I_{ds} and I_L at f_{sw} of 200 kHz in a series resonant inverter. A detailed waveforms during the switching transient, indicated by a rectangle in Fig. 4 a), is depicted in Fig. 4 b). It should be noted that these waveforms are recorded at a gate voltage of + 20 V / - 5 V and a gate resistance of 2.85 Ω.

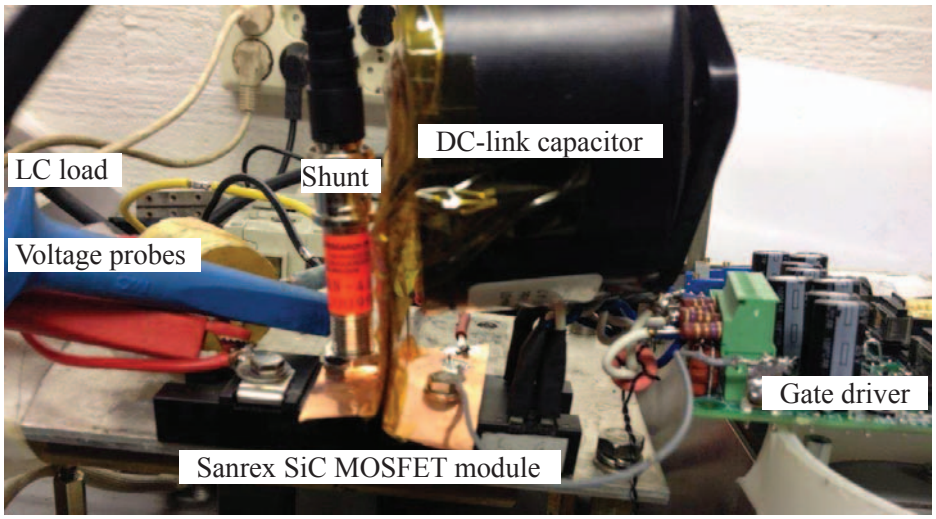

Fig. 3: Laboratory setup with low inductive dc-link. The drain current is measured by a high bandwidth, low inductive shunt, and the drain voltage is measured by a high bandwidth differential probe.

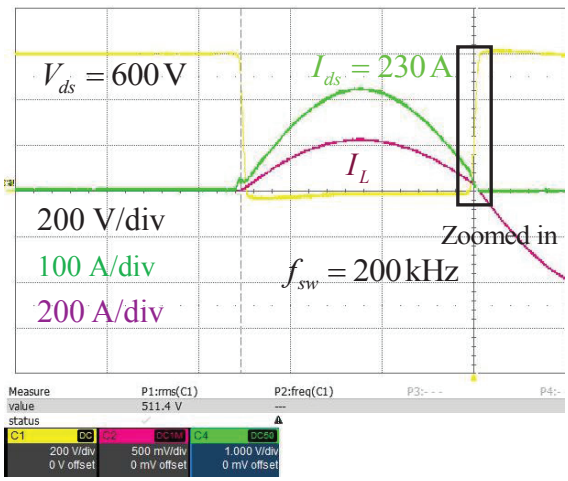

(a) Oscilloscope waveform for a half-bridge inverter.

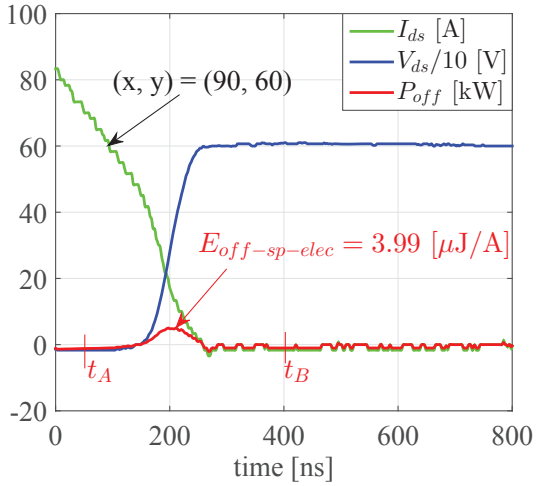

(b) Rectangular part in Fig. a) is zoomed in to compute loss.

Fig. 4: a) A sample of soft switching waveform at 600 V dc-link voltage, 230 A peak drain current and a switching frequency of 200 kHz. b) A detailed (zoomed in) view of a turn-off transient.

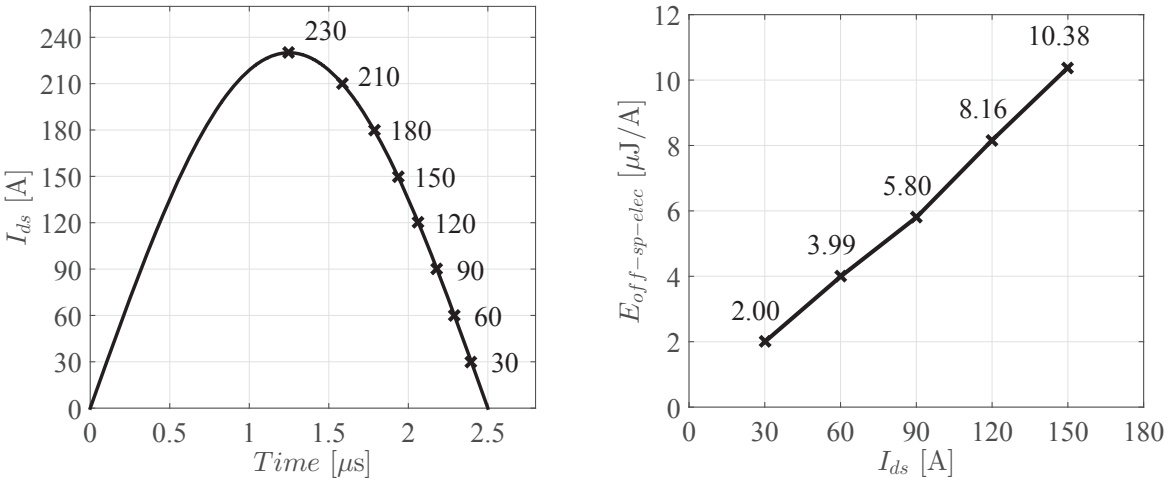

(a) Definition of turn-off current during soft switching.

(b) Turn-off switching loss at varying load current.

Fig. 5: a) Definition of the turn-off current and b) measured loss during soft switching.

Integrating the turn-off power (P_{off}) curve from t_A to t_B as indicated in Fig. 4 b), the specific turn-off loss per switch ($E_{off-sp-elec}$) is computed and is found to be 3.99 μJ/A at a switching current of 60 A. In order to acquire a full overview of switching losses at different current levels, the peak value of load current is fixed at 230 A and the turn-off instants are varied (by adjusting the blanking time), as defined in Fig. 5 a). Eventually, $E_{off-sp-elec}$ versus I_{ds} is plotted in Fig. 5 b). Depending on I_{ds}, $E_{off-sp-elec}$ varies from 2 μJ/A to 10.38 μJ/A.

3.2 Calorimetric loss measurement in a full-bridge resonant inverter

A schematic diagram of the experimental setup with a full-bridge resonant inverter for induction heating application is depicted in Fig. 6. The abbreviations used in the schematic are as follows. I_{dc}: dc-link current, V_{dc}: dc-link voltage, V_{out}: output voltage and I_{out}: output current. A full PWM control scheme is employed with a goal to measure the losses of the inverter part only. High frequency current is induced in the coil or inductor so that the metallic piece can be heated. The switching frequency is fixed to 187 kHz while the inverter losses are measured calorimetrically at different input power levels ranging from 30 kW to 78 kW.

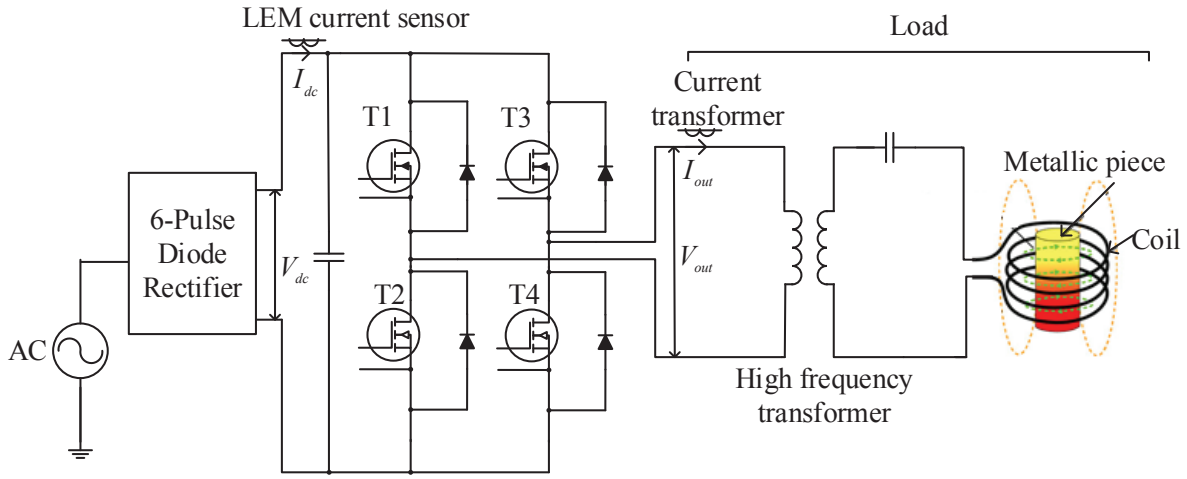

Fig. 6: A complete schematic diagram of the experimental setup for induction heating application. Input power of the inverter is measured in the dc-link (V_{dc} is measured by a precision voltmeter and I_{dc} by LEM current sensor) and the loss is measured using calorimetric method.

The main requirements in a soft switching inverter are addressed in this subsection. First, the low R_{dson} is desirable as it results in low conduction loss. Second, a majority carrier device (MOSFET) is preferred over a minority (IGBT) one because of two reasons. First, the latter possesses tail current during turn-off, which has strong dependency on temperature, and thereby causes more loss. Second, the on-state loss of this device not only increases with increase in junction temperatures, but also with increase in switching frequency [10, 14]. Since a long time, the Si IGBTs have taken the market in 1.2 kV and 1.7 kV class because Si MOSFETs in such voltage range have higher conduction losses. However, the arrival of SiC MOSFETs has opened new opportunities replacing Si IGBTs in same voltage range or even in higher voltage range [7].

A low inductive dc-link busbar is constructed with a stripline-terminated capacitor as depicted in Fig. 7, as it is important to have low inductive switching loop to maintain the safety particularly during the failure. It is clearly seen that the space occupied by the power switches is smaller compared to that by the gate driver. For a fair comparison, the same gate driver board as used during the electrical loss measurement method is employed during the calorimetric method. As mentioned in the previous subsection, the equal gate voltage (+ 20 V / - 5 V) and gate resistance (2.85 Ω) are maintained in each hardware setup. Additionally, the gate driver board is located at similar distances in each method which is clearly visible in Fig. 3 and Fig. 7.

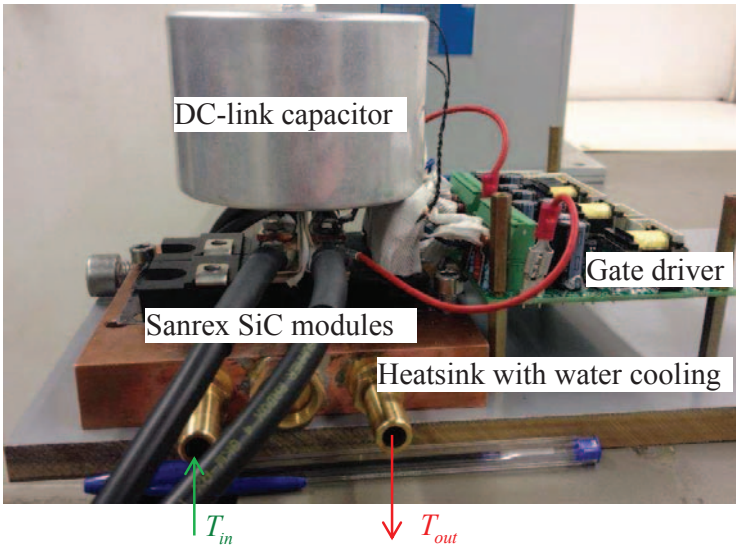

Fig. 7: A part of the experimental setup showing low inductive busbar connection for a full-bridge inverter along with water-cooled heatsink in order to facilitate the calorimetric loss measurement. Gate driver is located at similar distance as in electrical measurement method for a fair comparison of losses.

Table II: Summary of the measured parameters for three different input powers indicated by ”cases”.

Measured parameters	Case 1	Case 2	Case 3
I_{dc} (A)	55.8	120.8	142.8
V_{dc} (V)	543	546	545
I_{out} (A)	126	136	160.3
T_{in} (°C)	16.2	14.6	15
T_{out} (°C)	17.8	16.6	17.5
m (g/min)	3.124	2.990	2.990

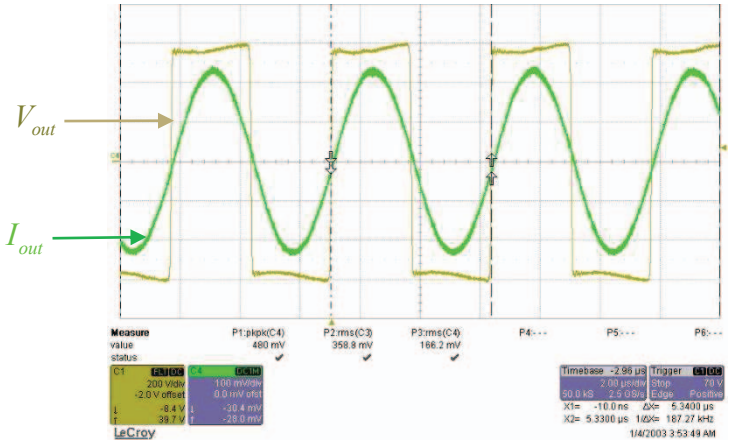

Fig. 8: A sample of oscilloscope waveforms are illustrated showing an inverter output voltage and current with full PWM control scheme. Gate voltage (+ 20 V / - 5 V) and gate resistance (2.85 Ω) are stringently kept equal in each of the loss measurement methods.

The summary of various electrical parameters, namely, I_{dc}, V_{dc}, and I_{out}; thermal parameters, namely, inlet and outlet temperatures of water (T_{in} and T_{out} respectively); and mass of water (m) are recorded for three different input power levels, and are listed in Table II as three different cases. The oscilloscope waveforms with the output voltage and current is displayed in Fig. 8.

Table III presents the summary of the calculated parameters for three cases. Using Equation 1 to 7, corresponding parameters in each row are computed. The abbreviations used in the equations are as follows. P_{in}: input power of inverter, Q: total power loss of inverter, s: specific heat capacity of water (4.186 $J/g/°$C), η: efficiency of inverter, P_{cond}: conduction power loss per switch, P_{sw}: switching power loss per switch, $E_{off-sp-calori}$: specific turn-off energy loss per switch, and ΔT: temperature rise from junction to case. For maintaining an adequate accuracy of measurement, the flow rate of water is maintained low. The measured efficiency of the inverter is about 99 % in all cases. For a maximum input power case (Case 3 in Table III), the conduction loss per switch is 89.93 W with R_{dson} being 7 $m\Omega$ (at the operating temperature) and the temperature rise is 15.64 °C (at the given R_{thjc} of 0.120 °C/W).

Table III: Summary of the calculated parameters for three different input powers.

Calculated parameters	Case 1	Case 2	Case 3	Equations	Eq. no.
P_{in} (kW)	30.29	65.97	77.82	$P_{in} = V_{dc} \cdot I_{dc}$	1
Q (W or J/s)	348.70	417.2	521.5	$Q = m \cdot s \cdot (T_{out} - T_{in})$	2
η (%)	98.84	99.36	99.33	$\eta = \frac{P_{in} - Q}{P_{in}}$	3
P_{cond} (W)	55.56	64.73	89.93	$P_{cond} = \left(\frac{I_{out}}{\sqrt{2}}\right)^2 \cdot R_{dson}$	4
P_{sw} (W)	31.61	39.56	40.44	$P_{sw} = \frac{Q}{4} - P_{cond}$	5
$E_{off-sp-calori}$ (μJ/A)	2.80	3.50	3.60	$E_{off-sp-calori} = \frac{P_{sw}}{f_{sw} \cdot I_{ds}}$	6
ΔT (°C)	10.46	12.51	15.64	$\Delta T = R_{thjc} \cdot \frac{Q}{4}$	7

Note that, $E_{off-sp-calori}$ is calculated for a drain current of 60 A for all three cases.

Table IV: Comparison of calorimetrically measured loss with regard to electrically measured loss.

Calculated parameters	Case 1	Case 2	Case 3	Remarks
$E_{off-sp-elec}$ (μJ/A)	3.99	3.99	3.99	from electrical measurement for I_{ds} of 60 A
$E_{off-sp-calori}$ (μJ/A)	2.80	3.50	3.60	from calorimetric measurement Table III
$\%_{diff}$ (%)	29.82	12.28	9.77	$\%_{diff} = \frac{E_{off-sp-elec} - E_{off-sp-calori}}{E_{off-sp-elec}} \cdot 100$

4 Discussion

Table IV shows the percentage difference between the specific turn-off energy loss per switch measured by electrical and calorimetric methods taking electrical method as a reference. This difference is higher by 9.77 % to 29.82 %, (depending on the inverter input power), as indicated in the last row of Table IV. It should be mentioned that the gate driving waveforms are maintained similar during each methods. Following are the reasons causing the discrepancies between the two measurement methods.

a) First, during the electrical measurement in laboratory, the drain current (summation of the current passed through the MOSFET channel and the current diverted for charging the output capacitance) and the drain voltage are measured using high bandwidth probes and oscilloscope. After compensating for the possible probe delays, these waveforms are multiplied together to compute power loss. Then, the power curve is integrated for the defined time limits to obtain the switching energy loss. The details about this procedure is explained in [15]. However, the real power loss in MOSFET is accounted by the channel current only and not the summation (drain current mentioned earlier). The summation of the currents was used while calculating the power loss because the MOSFET channel current cannot be measured separately in lab. This approach of measurement overestimates the switching energy loss because the current that goes for charging of the device output capacitor does not generate any Joule heating and should not be accounted as a part of the turn-off switching loss. Thus, the actual device loss must be smaller than the electrically measured loss in lab. This is also illustrated through simulation using a physically based device modelling approach in [16, 17]. In such a simulation, there is possibility to measure the current shared by the MOSFET channel and the output capacitor separately.

b) Second, $\%_{diff}$ is calculated assuming the switching loss at 60 A, i.e., 3.99 μJ/A for all cases. However, during the calorimetric measurement method, the phase difference between V_{out} and I_{out} can be different for different loading conditions, i.e., the minimum switching current during turn-off can vary.

c) Third, during the calorimetric loss measurement method, the total heat dissipated in the inverter circuit is measured which incorporates both conduction and switching losses as well as losses in other circuit components such as free-wheeling diode and layouts. In this work, the switching loss is calculated by subtracting only the conduction loss from the total loss, i.e., the remaining factors contributing to losses are neglected. This leads to overestimation of switching loss.

In the converter made with SiC MOSFETs, the efficiency is high, i.e., loss is small. This demands the highly accurate probes and oscilloscopes during the electrical loss measurement method. Nonetheless, the calculated loss will be higher as a part of measured current flows through the MOSFET output capacitance which is wrongly associated with loss. During the calorimetric loss measurement method the highly accurate flow meter and thermocouple are needed. In spite of that, the measured loss will be

higher as the direct heat dissipated in an inverter is measured which includes losses in layout, and wires, making it difficult to study the individual loss contributing factors.

However, it should be pointed out that even though these wrongly associated losses are considered, the converter efficiency is in the range of 99 % which is an impressive figure. Thus, SiC MOSFETs are very promising components for next generation high frequency generators in resonant applications, particularly induction heating applications. This is owing to the fact that by increasing the switching frequency, the benefit of skin effect can be utilized for surface heating of relatively small parts or tubes with small diameters where only a thin layer of the surface should be hardened or welded.

5 Maximum achievable switching frequency

Taking R_{thjc} of 0.12 °C/W from Table I [4] and a chosen temperature rise of 20 °C (from calorimetric measurement ΔT is 15.64 °C for the input power of about 78 kW, so it is rounded up to 20 °C to provide safety margin), the maximum allowable total power dissipation is 20/0.12 = 167 W. With the switching loss as input (as shown in Fig. 5) and conduction power loss of 100 W (the conduction loss is measured about 90 W for the input power of about 78 kW, therefore, it is rounded up to 100 W for safety margin), the maximum achievable switching frequency is computed by interpolation for 5 different switching currents (I_{ds1} to I_{ds5}). For the lowest current (I_{ds1} = 30 A), it is found to be 1.1 MHz and for the highest (I_{ds5} = 150 A), it is 43 kHz, as indicated in Table V. Evidently, this information can help decide to go in either of three directions; increase the switching frequency or increase the power of the inverter, or reduce the heatsink size.

Table V: Calculation of maximum possible switching frequency out of Sanrex SiC MOSFET module considering the maximum allowed conduction loss of 100 W and switching loss of 67 W.

Parameters	I_{ds1}	I_{ds2}	I_{ds3}	I_{ds4}	I_{ds5}	Remarks
I_{ds} (A)	30	60	90	120	150	Switching current
$E_{off-sp-elec}$ (μJ/A)	2	3.99	5.8	8.16	10.38	Input from Fig. 5
E_{off} (mJ)	0.06	0.2394	0.5220	0.9792	1.557	$E_{off} = E_{off-sp-elec} \cdot I_{ds}$
f_{sw} (kHz)	1100	277	130	68	43	Interpolated frequency

6 Conclusion

The major conclusions from this work are:

i) A resonant full-bridge inverter with SiC MOSFETs showed an efficiency of about 99.3 % at a switching frequency of about 200 kHz, using a calorimetric loss measurement method.

ii) The losses measured by an electrical method is higher by 9.77 % to 29.82 %, depending on the inverter input power, with reference to calorimetric method. Three possible reasons creating these differences are: First, the drain current through the MOSFET during electrical measurement is smaller than the measured value, because a part of the measured current is charging the MOSFET output capacitance. Second, the percentage difference between the electrical and calorimetric losses are calculated considering the constant phase difference in all the cases. However, when the loading changes this phase will be different and so does the switching current. Third, the factors causing losses such as layouts, and wires are neglected.

iii) The maximum possible switching frequency is calculated to be between 43 kHz and 1.1 MHz depending on the switching current. This insight can be utilized to increase the switching frequency, increase the output power or to reduce the heatsink size.

References

[1] ”CAS120M12BM2 Datasheet,” Cree, Inc., 2014.
[2] ”BSM120D12P2C005 Datasheet,” Rohm, Inc., 2014.
[3] ”SKM400GB125D Datasheet,” Semikron, Inc., 2007.
[4] ”FCA150XB120 (DS1) Preliminary Datasheet,” Sansha Electric Mfg. Co., Ltd, 2014.
[5] K. Vechalapu, S. Bhattacharya, E. VanBrunt, S. H. Ryu, D. Grider, and J. Palmour, ”Comparative Evaluation of 15 kV SiC MOSFET and 15 kV SiC IGBT for Medium Voltage Converter under Same dv/dt Conditions,” IEEE Journal of Emerging and Selected Topics in Power Electronics, vol. PP, pp. 1-1, 2016.
[6] S. Tiwari, O. -M. Midtgård, and T. M. Undeland, ”SiC MOSFETs for future motor drive applications,” in 2016 18th European Conference on Power Electronics and Applications (EPE’16 ECCE Europe), 2016, pp. 1-10.
[7] S. Tiwari, O. -M. Midtgård, and T. M. Undeland, ”Comparative Evaluation of a Commercially Available 1.2 kV SiC MOSFET Module and a 1.2 kV Si IGBT Module ” in Industrial Electronics Society, IECON 2016 - 42nd Annual Conference of the IEEE, 2016.
[8] C. Cases, J. Jordan, J. M. Magraner, V. Esteve, E. Dede, E. Sanchis, et al., ”Characterization of IGBT devices for use in series resonant inverter for induction heating applications,” in Power Electronics and Applications, 2009. EPE ’09. 13th European Conference on, 2009, pp. 1-8.
[9] D. Rothmund, D. Bortis, and J. W. Kolar, ”Accurate transient calorimetric measurement of soft-switching losses of 10kV SiC MOSFETs,” in 2016 IEEE 7th International Symposium on Power Electronics for Distributed Generation Systems (PEDG), 2016, pp. 1-10.
[10] J. K. Johansen, F. Jenset, and T. Rogne, ”Characterization of high power IGBTs with sinewave current,” IEEE Transactions on Industry Applications, vol. 30, pp. 1142-1148, 1994.
[11] M. Uchida, N. Horikawa, K. Tanaka, K. Takahashi, T. Kiyosawa, M. Hayashi, et al., ”Novel SiC power MOSFET with integrated unipolar internal inverse MOS-channel diode,” in Electron Devices Meeting (IEDM), 2011 IEEE International, 2011, pp. 26.6.1-26.6.4.
[12] ”Current Viewing Resistor (CVR),” T & M Research Products, Inc.
[13] S. Tiwari, O. -M. Midtgård, and T. M. Undeland, ”Design of low inductive busbar for fast switching SiC modules verified by 3D FEM calculations and laboratory measurements,” in 2016 IEEE 17th Workshop on Control and Modeling for Power Electronics (COMPEL), 2016, pp. 1-8.
[14] P. Ranstad, H. P. Nee, J. Linnr and D. Peftitsis, ”An Experimental Evaluation of SiC Switches in Soft-Switching Converters,” in IEEE Transactions on Power Electronics, vol. 29, no. 5, pp. 2527-2538, May 2014.
[15] S. Tiwari, J. K. Langelid, O. -M. Midtgård, and T. M. Undeland, ”Hard and soft switching losses of a SiC MOSFET module under realistic topology and loading conditions,” in 2017 19th European Conference on Power Electronics and Applications (EPE’17 ECCE Europe), 2017, pp. 1-10.
[16] Y. Xiong, S. Sun, H. Jia, P. Shea and Z. John Shen, ”New Physical Insights on Power MOSFET Switching Losses,” in IEEE Transactions on Power Electronics, vol. 24, no. 2, pp. 525-531, Feb. 2009.
[17] X. Li, L. Zhang, S. Guo, Y. Lei, A. Q. Huang and B. Zhang, ”Understanding switching losses in SiC MOSFET: Toward lossless switching,” 2015 IEEE 3rd Workshop on Wide Bandgap Power Devices and Applications (WiPDA), Blacksburg, VA, 2015, pp. 257-262.